Available online at www.sciencedirect.com
ScienceDirect
Trans. Nonferrous Met. Soc. China 25(2015) 628−639
Transactions of Nonferrous Metals Society of China
www.tnmsc.cn

# Preparation of potassium salt with joint production of spherical calcium carbonate from sintering dust

Guang ZHAN, Zhan-cheng GUO

State Key Laboratory of Advanced Metallurgy, University of Science and Technology Beijing, Beijing 100083, China

Received 31 March 2014; accepted 17 November 2014

**Abstract:** Several physical and chemical detection methods were used to study the basic properties of sintering dust (ESP dust) collected from Baogang Steel Corporation. The result shows that the major constituents of the ESP dust are KCl, NaCl, $Fe_2O_3$ and $Fe_3O_4$. Water leaching experiment on the sintering dust shows that KCl in the ESP dust can be separated and recovered by water leaching and fractional crystallization. Component analysis of leaching solution indicates that the massive calcium sulfate in the leaching solution should be removed first in order to obtain the pure potassium salt. In order to provide theoretical guidance to inhibit the dissolution of calcium ions from the sintering dust, the water leaching experiment of ESP dust and the dissolution behavior of $CaSO_4$ in the potassium chloride, sodium chloride, potassium sulfate and their mixed salt solution were studied. It is found that, a lower liquid−solid ratio should be chosen in the leaching process to inhibit the dissolution of calcium sulfate dehydrate. Using sodium carbonate solution as a precipitating agent, the influences of the concentration of sodium carbonate solution, reaction temperature, stirring speed and equilibrium time on the preparation of the spherical calcium carbonate were studied. Spherical calcium carbonate with good dispersing performance and grain size distribution in nanometer range of less than 10 μm was obtained. Furthermore, a potassium recovery process with joint production of spherical calcium carbonate was designed. This process is technically viable and considerable in economic benefit.

**Key words:** sintering dust; potassium salt; recovery experiment; spherical $CaCO_3$

## 1 Introduction

Potassium chloride is one of the most important potassium fertilizers, and also is the major raw material of non-chloride potassium fertilizers. In the first ten months of 2012, the potash fertilizer import in China increased by 9.7% to 5.714 million tons (pure KCl) [1] and the CFR (Cost and Freight) price increased by 23.7% to 470 dollars per ton [2]. The main reasons for the increasing price of the potash are the increase of the consuming capacity of potash fertilizer as well as the decrease of its production in China. To meet its requirement, a potassium chloride plant with a capacity of 10000 t/a sintering dust has been built in Tangshan, based on a national invention patent for producing potassium chloride from sintering dust [3]. Water leaching experiment on the sintering dust collected from Baogang Steel Corporation shows that KCl, NaCl, $K_2SO_4$ and $CaSO_4$ are the four major constituents in the water leaching solution [4,5]. There would be an adverse effect on the quality of KCl product, if the mixture leaching solution was directly evaporated and crystallized without removing $CaSO_4$ first. Moreover, the incrustant of calcium sulfate would cause a series of problems during the industrial crystallization processes, including reducing the heat transfer efficiency and corroding the equipment significantly [6]. Therefore, it is indispensable to remove $Ca^{2+}$ before evaporation procedures for the industrial process of producing potassium from sintering dusts.

It can be briefly summarized that the $Ca^{2+}$ removing methods from the salt brine are caustic soda−soda ash method, lime−soda ash method and lime−sodium sulfate-flue gas method, and the common principle is the transformation of $Ca^{2+}$ into $CaCO_3$ by $CO_3^{2-}$ [7,8]. There are three kinds of calcium carbonate crystal forms which are calcite, aragonite and vaterite. The most difficult obtained and important used of them is spherical calcium carbonate with vaterite crystal form. Spherical calcium

**Foundation item:** Projects (2012AA062502, 2012AA06A118) supported by the National High-tech Research and Development Program of China
**Corresponding author:** Zhan-cheng GUO; Tel: +86-10-82375041; E-mail: zcguo@metall.ustb.edu.cn
DOI: 10.1016/S1003-6326(15)63646-9

carbonate powder material is widely used in ink, paint and other industries due to its large surface area, low specific gravity, good dispersion and solubility [9,10]. Since the crystal morphology of the calcium carbonate has great influence on its physical and chemical properties, the research hotspot of the production of calcium carbonate, especially the size-uniform spherical calcium carbonate, is focused on the using of organics as a regulating agent to control the crystal shape, type and size [11−17]. This highly influential template regulation agent significantly complicates the spherical calcium carbonate preparation method. However, direct preparation of calcium carbonate without adding crystalline controller is rarely reported.

In this work, in order to provide theoretical guidance to inhibit the dissolution of calcium ions from the sintering dust, the water leaching of ESP dust and the effect of potassium chloride, sodium chloride, potassium sulfate and their mixed salt on the solubility of $CaSO_4{\cdot}2H_2O$ were studied. Secondly, sodium carbonate was used as a precipitant to remove the calcium ions and the spherical $CaCO_3$ was obtained as a by-product. Thirdly, a potassium recovery process with joint production of spherical calcium carbonate was designed.

## 2 Experimental

### 2.1 XRF, XRD and SEM analysis

The structural characterization of ESP dust was performed with X-ray fluorescence spectrometer (XRF−1800, Japan), X-ray diffraction (M21, MAC, Japan) and SEM (Cambridge S−360, UK) analysis. X-ray patterns of samples powdered to 48 μm were obtained in the $2\theta$-range from 10° to 90° with a scan step of 0.05°, and fixed counting time of 1 s for each step. The patterns were analyzed by Search-match software. Samples of the dust were examined with a scanning electron microscope (SEM) and X-ray mapping (Tracor Northern, USA) via SEM−EDS to gain a better understanding of the ESP dust.

### 2.2 Leaching solution component analysis

A certain amount of ESP dusts were added into the deionized water in a conical flask and stirred for 1 h (the liquid−solid ratio was 80:1 and 1:1). After that, the leaching solution was filtered and evaporated to crystals. The concentrations of the major water-soluble particle species ($K^+$, $Na^+$, $Ca^{2+}$, $Mg^{2+}$, $Al^{3+}$, $Cl^-$, $SO_4^{2-}$, $NO_3^-$, $Br^-$, $F^-$, and $PO_4^{3-}$) in the crystals were determined by an ICP-AES (Perkin-Elmer OPTIMA 3000, USA) and IC (Metrohm 792 Basic, Switzerland).

### 2.3 Removal and recovery of calcium

Using sodium carbonate as a precipitant, the calcium ion dissolved in the leaching solution could be removed by converting into calcium carbonate precipitation. Firstly, according to the composition of the leaching solution of No. 2 experiment listed in Table 3, a mixed salt solution was made and added into a three mouth flask, which was placed in the super thermostatic bath. Then sodium carbonate solution was added into the flask through a peristaltic pump with certain flow rate to react with the calcium ions. During the process of precipitating reaction, the electric conductivity and concentration of calcium ions in the solution were determined by a conductivity meter (DDS−11A, INESA, China) and ICP-AES, respectively. At last, precipitated particles were obtained by washing, filtrating and drying. The phase composition of the precipitated particles was qualitatively characterized by X-ray diffraction (M21, MAC, Japan). To investigate the shape and particle size of the precipitated particles, a scanning electron microscope (JSM−6701F, Japan) was used.

## 3 Results and discussion

### 3.1 Analysis of ESP dust

The content of the ESP dust detected by X-ray fluorescence spectroscopy is shown in Table 1. It can be seen that the main metal elements in the sintering dust are Fe, K, Ca and Na with the total mass fraction of their oxides up to 70%.

**Table 1** XRF results of ESP dust (mass fraction, %) [5]

| $Fe_2O_3$ | $K_2O$ | $SiO_2$ | $SO_3$ | ZnO | CaO | $Al_2O_3$ |
|---|---|---|---|---|---|---|
| 43.3 | 14.71 | 2.84 | 5.86 | 0.09 | 7.67 | 0.73 |
| $Na_2O$ | MgO | Cl | PbO | F | $P_2O_5$ | |
| 4.36 | 1.8 | 14.53 | 1.3 | 1.82 | 0.08 | |

Figure 1 shows SEM−EDS and XRD results of the ESP dust. It is clearly seen that the major constituents of the ESP dust are KCl, NaCl, $Fe_2O_3$ and $Fe_3O_4$. The strong diffraction peaks of potassium chloride illustrate a high content in the ESP dust. The SEM−EDS results in Figs. 1(c) and (d) show further proof of the presence of KCl particles in the ESP dust. The XRD pattern of the elements of K and Cl shows that the particles at the point *A* are KCl particles. This indicates that the potassium exists mainly in the form of KCl in the ESP, therefore Cl and K always have the same distribution.

### 3.2 Leaching experiment

In order to discuss the possibility of potassium recycling, a water leaching experiment was carried out on the sintering dust. The main components of the water-washed ESP dust are listed in Table 2, which shows that there is almost no $K^+$, $Na^+$ or $Cl^-$ left in the

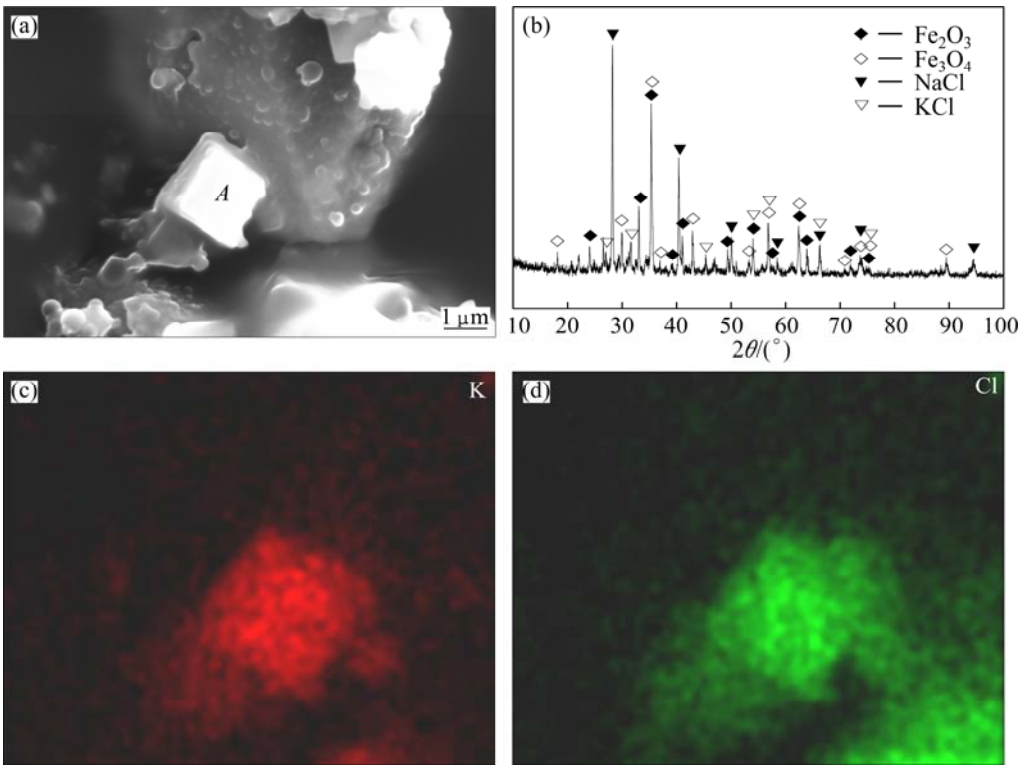


**Fig. 1** SEM-EDS mapping of K and Cl and XRD pattern of ESP dust [5]: (a) SEM image; (b) XRD pattern; (c) EDS mapping of K; (d) EDS mapping of Cl

**Table 2** XRF results of water-washed ESP dust (mass fraction, %) [5]

| $Fe_2O_3$ | $K_2O$ | $SiO_2$ | $SO_3$ | ZnO | CaO | $Al_2O_3$ |
|---|---|---|---|---|---|---|
| 67.46 | 0.35 | 10.04 | 1.45 | 0.17 | 10.24 | 1.98 |
| $Na_2O$ | MgO | Cl | PbO | F | $P_2O_5$ | |
| 0.42 | 4.3 | 0.13 | 2.04 | − | 0.22 | |

water-washed dust. In comparison with the XRF results of the ESP dust (see Table 1), it is clearly found that the potassium resource can be separated from the sintering dust by water leaching.

The ICP-AES and ion chromatography (IC) results of the crystalline are shown in Table 3. As it can be seen, the main components of the crystalline are potassium salt and sodium salt, wherein more than 70% of the crystalline is potassium salt and over 23% is sodium salt. Different liquid−solid ratios cause the yield and the component of the crystal substance different. When the liquid−solid ratio changes from 1:1 to 80:1, the content of potassium salt remains approximately the same, yet the calcium salt content surges from 0.97% to 4.12%. The additional leaching water does not significantly increase the potassium content in the crystal substance, but raise the calcium sulfate ions content in the crystal substance and the additional fee in the evaporating process.

Besides, the contents of calcium ions in both crystal substances mentioned above are different. From the result listed in Table 3, it is computed that ions product of $Ca^{2+}$ and $SO_4^{2-}$ ions in the leaching solution obtained in experiment No.2 was $1.594\times10^{-3}$, which is much higher than the solubility product constant ($K_{sp}$) of $CaSO_4$ ($7.1\times10^{-5}$) [18]. The calcium and sulfate ions in the leaching solution exist as free ions rather than the $CaSO_4$ precipitates.

The main components of the leaching solution of the sintering dust are potassium chloride, sodium chloride, potassium sulfate and calcium sulfate. The calcium sulfate in the leaching solution is much more soluble than that in the pure water. In order to obtain the pure potassium chloride and reduce the corrosion of the evaporating crystallizer, it is important to understand the solubility of calcium sulfate in the sintering leaching process. Thus, some improved processes can be used to reduce the solubility of calcium sulfate in the sintering dust leaching process.

In order to provide theoretical guidance for the removal of calcium ions from leaching solution, the solubility laws of the calcium sulfate in the potassium chloride, sodium chloride, potassium sulfate and their mixture were studied and shown in Fig. 2. The point of abscissa value of 0 denotes the solubility of calcium sulfate dihydrate in pure water, whilst other points mean the solubility of calcium sulfate dihydrate in solution

**Table 3** Yield and composition of crystalline substance

| No. | Liquid−solid ratio | Crystalline recovery yield/% | Composition/% | | | | | | |
|---|---|---|---|---|---|---|---|---|---|
| | | | $SO_4^{2-}$ | $K^+$ | $Na^+$ | $Ca^{2+}$ | $Al^{3+}$ | $Pb^{3+}$ | $Cl^-$ |
| 1 | 80:1 | 18.56 | 16.99 | 36.41 | 5.34 | 4.12 | 0.002 | 0.0059 | 37.32 |
| 2 | 1:1 | 12.51 | 4.01 | 37.93 | 9.37 | 0.97 | 0.026 | 0.009 | 47.84 |

Recovery yield=(mass of crystalline/mass of initial powders) ×100%; Composition (X)=(mass of X/mass of crystalline)×100%, where X denotes some kinds of ions contained in the crystalline.

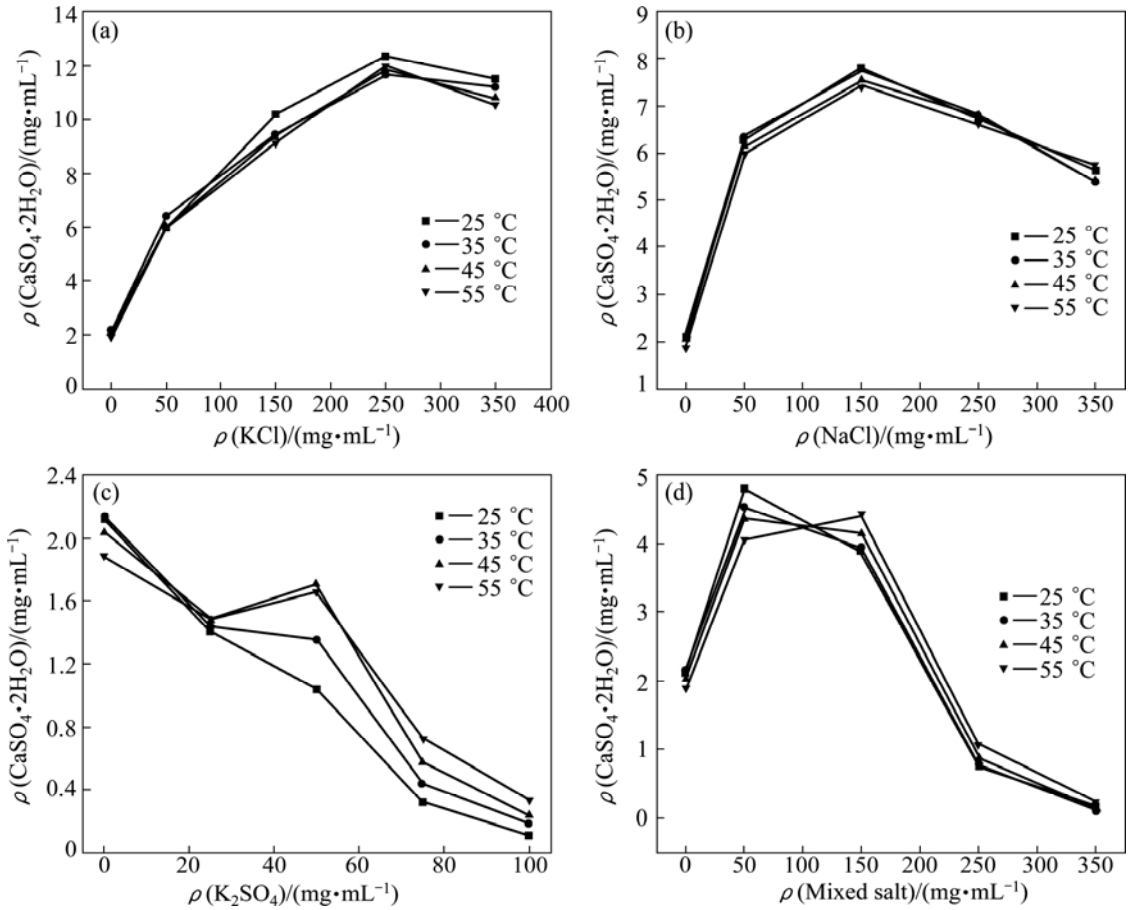


**Fig. 2** Solubility of $CaSO_4·2H_2O$ in salt solution: (a) In KCl solution; (b) In NaCl solution; (c) In $K_2SO_4$ solution; (d) In KCl−NaCl−$K_2SO_4$ solution

with a certain concentration of salt solution. As it can be seen, the solubility of calcium sulfate dihydrate increases sharply with the increasing concentrations of KCl (see Fig. 2(a)) and NaCl (see Fig. 2(b)). The concentration of $CaSO_4$ in KCl solution is over 6 times that in pure water (the point of abscissa value of 0). According to the Debye−Hukel ion-attraction theory [19], anions/cations are surrounded by lots of their counter-ions. In the high concentration solution of KCl (NaCl), $SO_4^{2-}$ ions are surrounded by $K^+$ ($Na^+$) ions while $Ca^{2+}$ ions are surrounded by $Cl^-$ ions. Consequently, $SO_4^{2-}$ and $Ca^{2+}$ are restrained by ionic atmosphere electrostatic forces of their counter-ions, which prevent them forming $CaSO_4$ precipitate. In other words, the dissolving rate of $CaSO_4$ is faster than its precipitating rate. Therefore, the solubility of $CaSO_4$ in KCl (NaCl) solutions is higher than that in pure water and increases with the concentration of KCl (NaCl) [20].

Figure 2(c) describes the relationship between concentration of sulfate ionic and the solubility of calcium sulfate dihydrate in aqueous potassium sulfate solution. It is notable that compared with the solubility of calcium sulfate in pure water (the points with the abscissa value of 0), it decreases sharply with potassium sulfate concentration increasing. This phenomenon can be explained by the common ion effect according to the following equation [21]:

$$CaSO_4=Ca^{2+}+SO_4^{2-},\ K_{sp}^{\Theta}=7.1\times10^{-5} \quad (1)$$

It can be calculated that the concentrations of $Ca^{2+}$ and $SO_4^{2-}$ of 100 mL saturated $CaSO_4$ solution are both $8.426\times10^{-3}$ mol/L in the standard state. But the

concentration of $Ca^{2+}$ can be significantly reduced to $7.05\times10^{-4}$ mol/L when 0.1 mol $K_2SO_4$ was added into the $CaSO_4$ saturated solution. The common ion effect of $SO_4^{2-}$ greatly inhibits the dissolution of calcium sulfate [22].

The solubility of calcium sulfate in KCl−NaCl−$K_2SO_4$ mixed salt solutions (mass ratio of KCl to NaCl to $K_2SO_4$=7:2:1) is shown in Fig. 2(d). It is found that low concentration of the mixed salt solution (less than 150 mg/mL) accelerates the dissolution of calcium sulfate dehydrate, while the high concentration (more than 150 mg/mL) inhibits its dissolution effectively. The observation is consistent with the results in Table 3, where the concentration of the mixed salt in No. 2 experiment is about 100 mg/mL and the concentration of $CaSO_4$ is higher that its solubility. The leaching solution has a higher salt content at a lower liquid−solid ratio due to the predominant role of common ion of sulfate on inhibiting the dissolution of calcium sulfate dehydrate.

The analysis results of the leaching solution and the solubility of $CaSO_4\cdot2H_2O$ in salt solutions indicate that, in order to obtain pure potassium chloride and reduce the cost of the evaporation process, a lower liquid−solid ratio should be chosen in the leaching process to inhibit the dissolution of calcium sulfate dehydrate. A low liquid−solid ratio not only inhibits the dissolution of calcium ions from the sintering dust, but also decreases the precipitant consumption in the precipitation process and saves energy consumption in the evaporation crystallization process.

### 3.3 Removal of calcium

The main components of the sintering dust leaching solution are KCl, NaCl, $K_2SO_4$ and $CaSO_4$, and the $Ca^{2+}$ can be removed from this solution by combining with $CO_3^{2-}$ to form $CaCO_3$ precipitate [7,8]. The preparation methods of spherical calcium carbonate by transforming the calcium sulfate into calcium carbonate were investigated.

The effect of sodium carbonate content on the removal rate of calcium ion was investigated. Conductivity is an indicator of the concentration of dissolved salts in the solution [23]. Figure 3 shows that the conductivity of the solution decreases significantly as the calcium carbonate precipitation reaction proceeds. Taking the typical conductivity curve in Fig. 3(d) as an example, the chemical reactions can be divided into the following five stages [23].

1) The solution was undersaturated during 0−1 min, and the conductivity of the solution increased as the

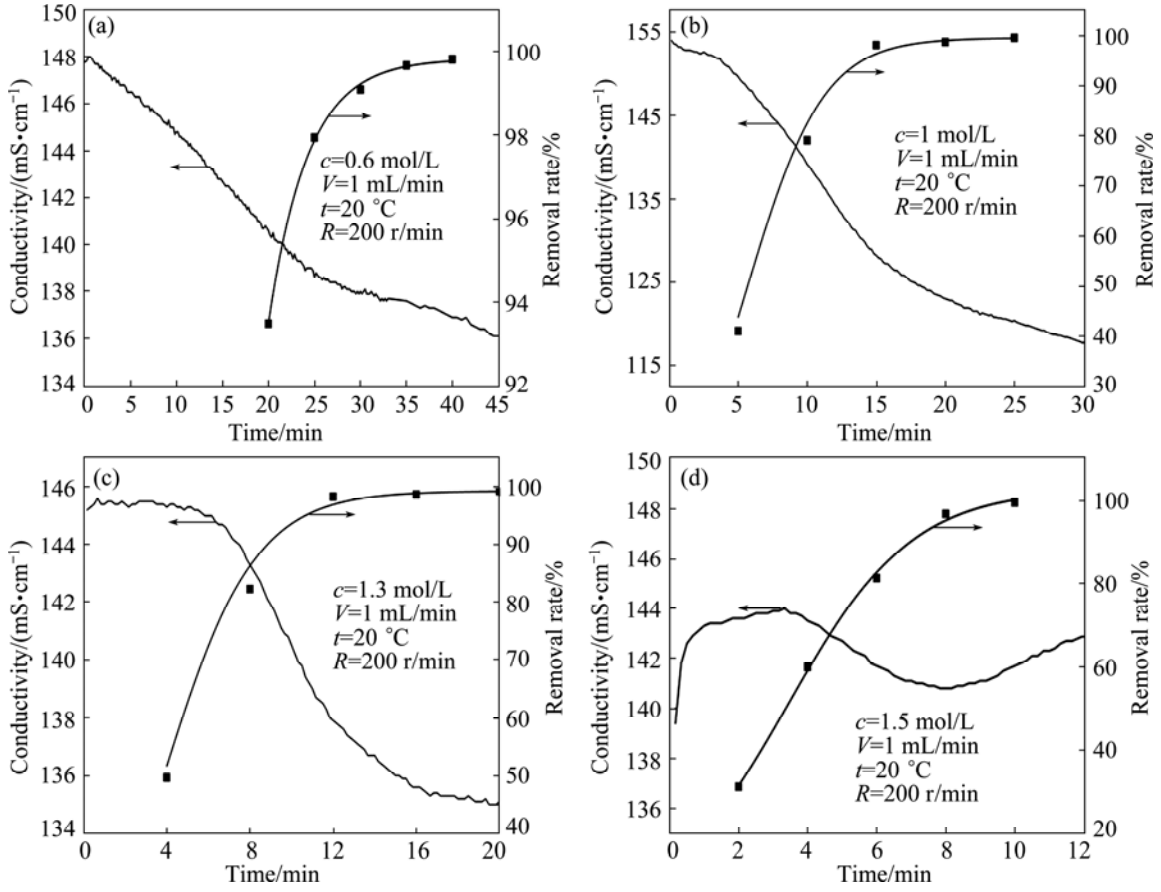


**Fig. 3** Effect of sodium carbonate concentration on calcium ion removal rate: (a) 0.6 mol/L; (b) 1.0 mol/L; (c) 1.3 mol/L; (d) 1.5 mol/L

$Na_2CO_3$ solution dropped, but almost no calcium carbonate was precipitated. This is because the total ion concentration of the mixed salt solution increased with the addition of $Na_2CO_3$, while the concentration of $Ca^{2+}$ and $CO_3^{2-}$ in the mixed salt solution was less than the solubility of $CaCO_3$ ($K_{sp}$) in this stage.

2) At 1 min, the solution reached saturation and the maximum of the conductivity was reached. The concentrations of $Ca^{2+}$ and $CO_3^{2-}$ in the mixed salt solution might be equal to $K_{sp}$ and calcium carbonate crystal nucleus appeared. Therefore, the concentration of the total ions in the solution reached the maximum as well as its conductivity.

3) 1−4 min is a stage called nucleation. As the $Na_2CO_3$ solution is added, the supersaturation of the $Ca^{2+}$ and $CO_3^{2-}$ increased, and the amount of $CaCO_3$ crystal increased through the $CaCO_3$ crystal spontaneous nucleation occurred. The increase in conductivity caused by the adding of $Na_2CO_3$ solution overwhelmed the decrease in conductivity caused by the formation of $CaCO_3$ molecules that the conductivity of the solution enhanced slowly.

4) 4−8 min is the precipitation stage. The $CaCO_3$ crystals grew larger into calcium carbonate clusters and precipitated out from the solution through collision and coalescence. The conductivity of solution decreased significantly as the total ion concentration of the solution reduced. The inflection point of the conductivity curve appeared around about 8 min, signaling the end of the $CaCO_3$ precipitation reaction.

5) 8−12 min is the last stage. With the addition of $Na_2CO_3$ solution, the calcium carbonate coated the surface of the measurement probe of the conductivity meter causing the sensitivity of the conductivity meter to decline and the conductivity of solution to increase.

The calcium removal curves in Fig. 3 indicate that the calcium ion can be removed completely by sodium carbonate. Based on the calculation of the dosage of sodium carbonate, the carbonate ions and calcium ions would be reacted completely under the mole ratio of 1:1, suggesting that it is effective to remove calcium ion with sodium carbonate.

### 3.4 Recovery of calcium

#### 3.4.1 Effect of sodium carbonate content on spherical $CaCO_3$ preparation

Figure 4 shows the SEM images of the calcium carbonate byproduct obtained under different concentrations of sodium carbonate solutions. It can be seen that the spherical crystal calcium carbonate exhibits a narrow size distribution and good dispersivity. The crystals are smooth and dispersive, with uniform particles smaller than 10 μm in size. The XRD results (see Fig. 5) reveal that these particles are calcite and vaterite almost without impurities. As the concentration of sodium carbonate solutions changes from 0.6 to 1.5 mol/L, the mass ratio of calcite to vaterite increases from 84:16 to 100:0.

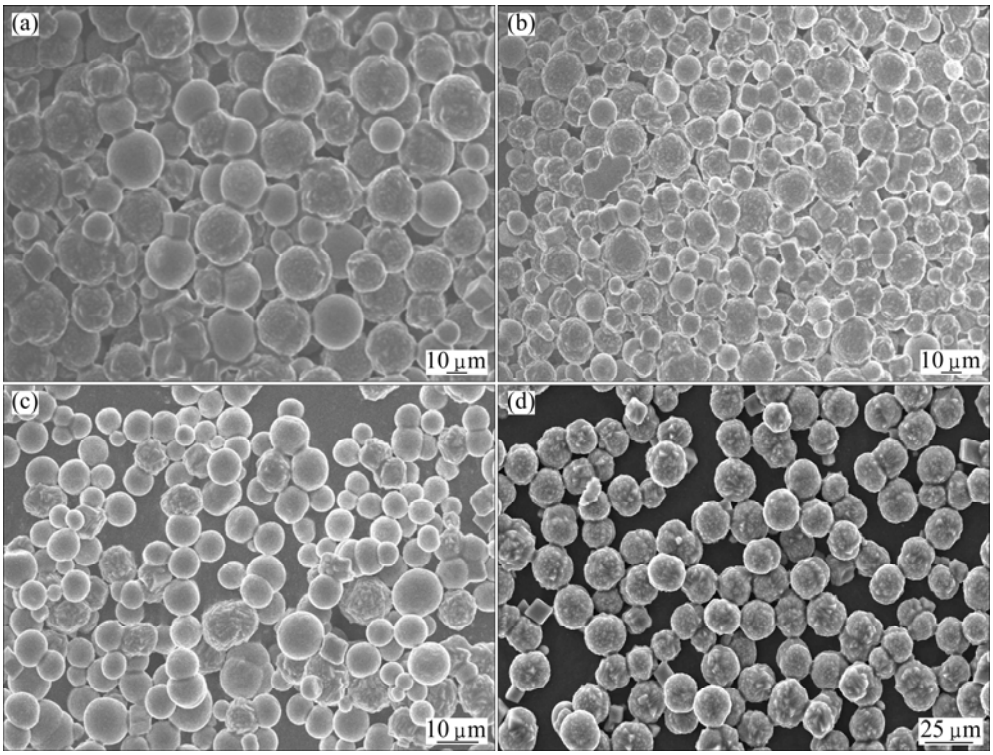


**Fig. 4** SEM images of obtained calcium carbonate with different concentrations of sodium carbonate: (a) 0.6 mol/L; (b) 1.0 mol/L; (c) 1.3 mol/L; (d) 1.5 mol/L (Flow rate 1 mL/min; Reaction temperature 20 °C; Stirring speed 200 r/min; Equilibrium time: 0 min)

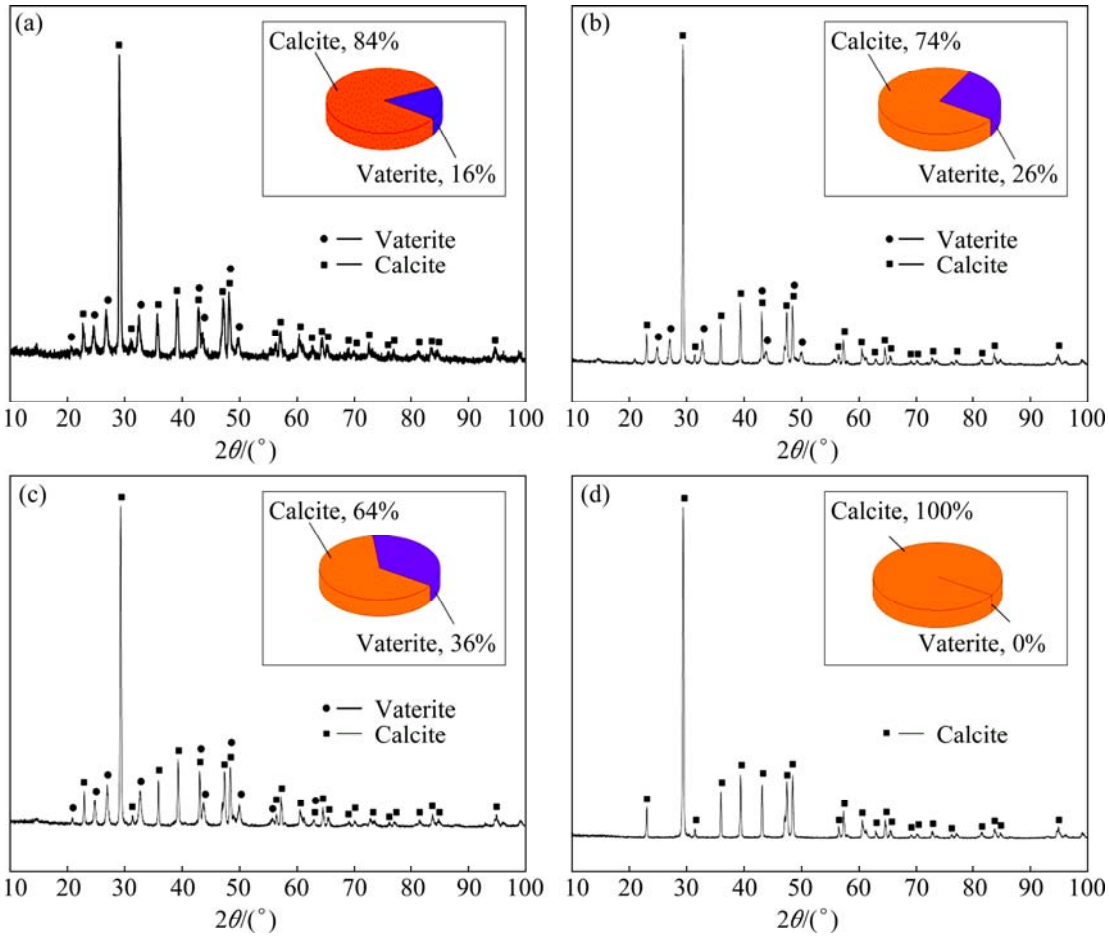


**Fig. 5** XRD patterns of obtained calcium carbonate with different concentrations of sodium carbonate: (a) 0.6 mol/L; (b) 1 mol/L; (c) 1.3 mol/L; (d) 1.5 mol/L (Flow rate 1 mL/min; Reaction temperature 20 °C; Stirring speed 200 r/min; Equilibrium time: 0 min)

It is found that spherical calcium carbonate with good dispersing performance and grain size distribution in nanometer range of less than 10 μm could be obtained easily by dropping $Na_2CO_3$ solution into the sintering dust leaching solution. Under the consideration of reaction time and the quality of the spherical calcium carbonate, the concentration of $Na_2CO_3$ solution was 1.3 mol/L.

3.4.2 Effect of reaction temperature on spherical $CaCO_3$ preparation

The effects of temperature on the crystal shape (SEM) and crystal form (XRD) of calcium carbonate are shown in Fig. 6. It is found that temperature has a great impact on the crystal shape and crystal form of calcium carbonate. At the temperature of 20 °C, the crystal shape of precipitated calcium carbonate is spherical, and the crystal form is a mixed form of calcite and vaterite. As the temperature increases, cube calcium carbonate begins to appear, and the size of vaterite calcium carbonate begins to shrink. When the temperature rises to 35 °C, the precipitated calcium carbonate transforms from spherical into cube completely. According to the solubility thermodynamics empirical formula of calcite and vaterite [24], the vaterite in solution is less stable than that of calcite, it is adverse to form the vaterite at higher reaction temperature. Therefore, spherical calcium carbonate is suggested to be prepared at lower reaction temperatures.

3.4.3 Effect of stirring speed on calcium removal and spherical $CaCO_3$ preparation

The stirring speed has a significant influence on the crystal shape and crystal form of calcium carbonate (see Fig. 7). As one of the important parameters to the crystal growth in crystal growth theories, the stirring intensity can strengthen the mixing of liquids. When the stirring speed increases from 200 to 600 r/min, the precipitated calcium carbonate crystal obviously shrinks in size and its surface becomes rougher. The higher stirring speed further enhances the positive impact on liquid−liquid mixing and chemistry reaction velocity [25]. The enhanced turbulent motion of the solution can increase the collisions probability among the calcium carbonate crystals, leading to more calcium carbonate crystal collision and agglomeration. As the reaction velocity accelerated, the unstable vaterite ($CaCO_3$) tends to transform into the stable calcite ($CaCO_3$).

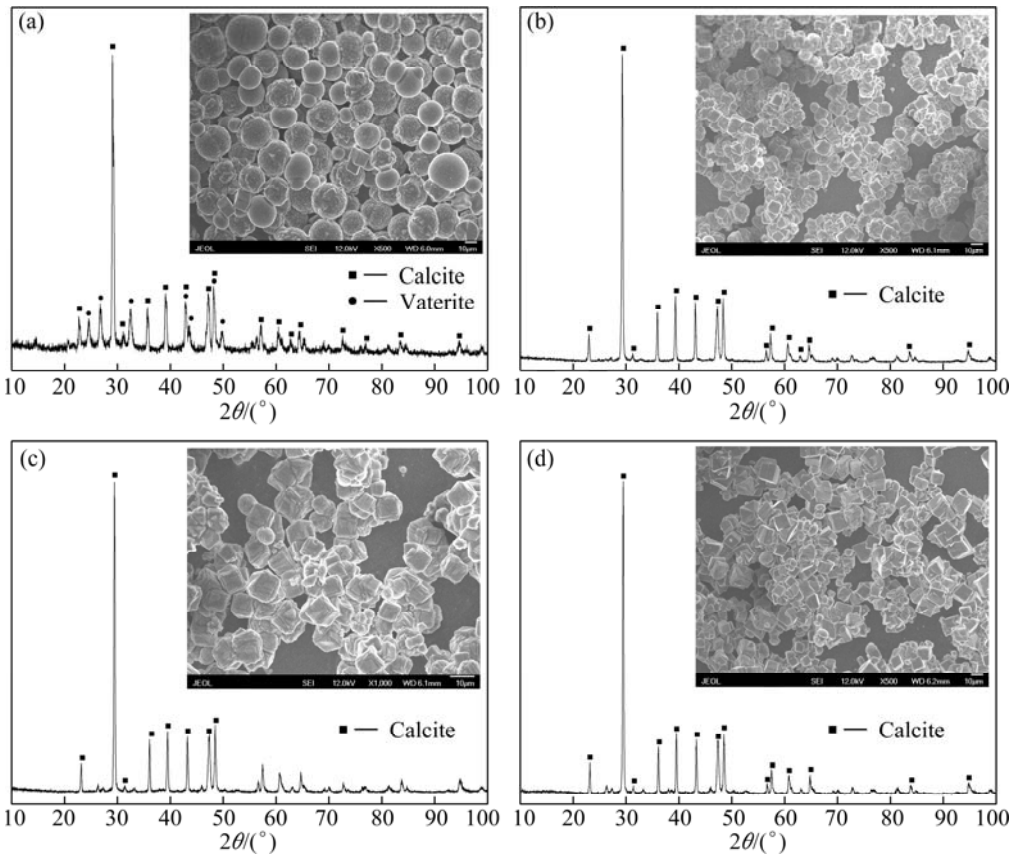


**Fig. 6** SEM images and XRD patterns of calcium carbonate at different temperatures: (a) 20 °C; (b) 25 °C; (c) 30 °C; (d) 35 °C (Concentration 0.6 mol/L; Flow rate 1 mL/min; Stirring speed 200 r/min; Equilibrium time: 0 min)

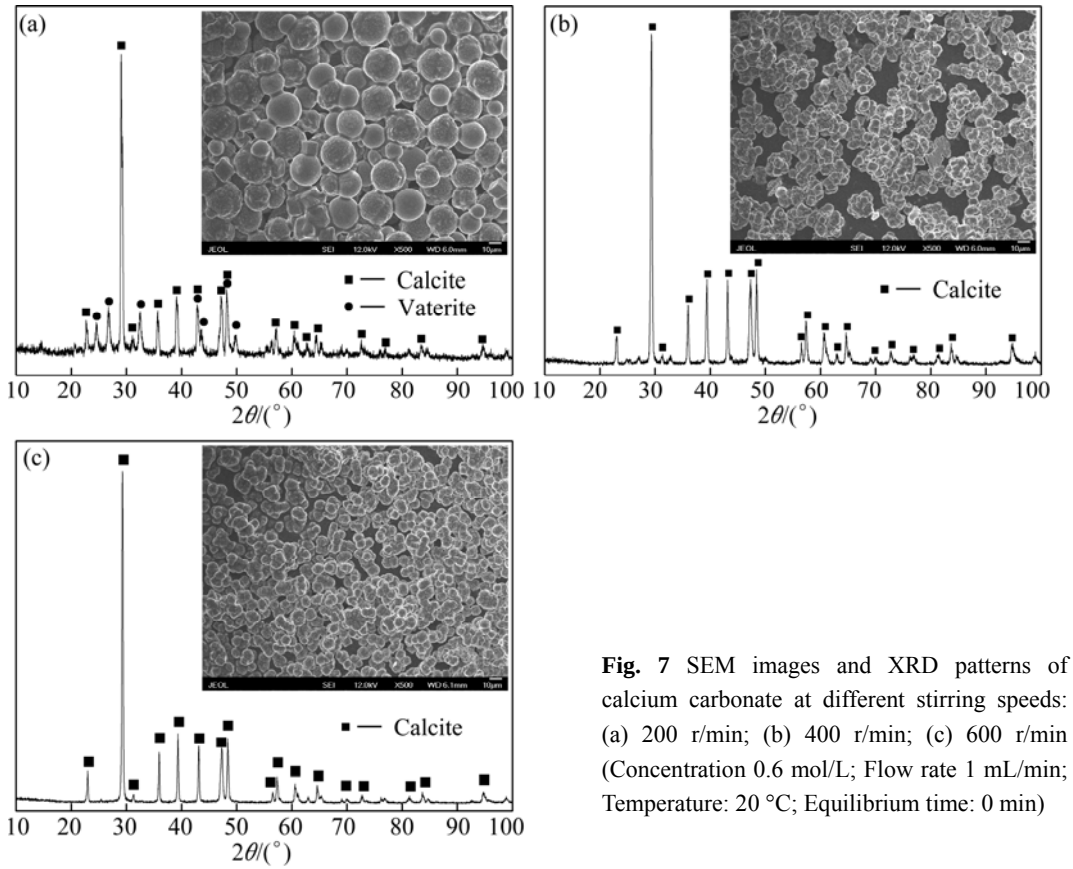


**Fig. 7** SEM images and XRD patterns of calcium carbonate at different stirring speeds: (a) 200 r/min; (b) 400 r/min; (c) 600 r/min (Concentration 0.6 mol/L; Flow rate 1 mL/min; Temperature: 20 °C; Equilibrium time: 0 min)

3.4.4 Effect of equilibrium time on calcium removal and spherical $CaCO_3$ preparation

The effect of reaction equilibrium time on the precipitated calcium carbonate particles was investigated and the results of SEM and XRD are shown in Fig. 8. With equilibrium time prolonging, the collisions probabilities among the calcium carbonate crystals increased and the calcium carbonates crystal agglomerated badly, until the unstable vaterite ($CaCO_3$) completely transformed into the stabled calcite ($CaCO_3$). Generally, the most unstable amorphous calcium carbonate was generated initially when the $Ca^{2+}$ reacted with $CO_3^{2-}$ ions, and then, with the reaction time prolonging, the metastable vaterite and aragonite and the most stable calcite were formed one by one [17].

3.4.5 Effect of $Na_2CO_3$ step-wise addition method on calcium removal and spherical $CaCO_3$ preparation

Although $Na_2CO_3$ solution offers a high removal rate of calcium ions, it will enlarge the volume of the target liquid that enhancing the energy consumption of the evaporation crystallization process [5]. In this section, the preparation of spherical $CaCO_3$ by-product using the $Na_2CO_3$ powders was investigated. The amount of $Na_2CO_3$ powders which is 1.2 times that of $CaSO_4$ in the processing liquid was divided into several share(s) and added into the processing liquid. It is clear from the XRD results (see Fig. 9) that the obtained calcium carbonate is calcite. Figure 9 reveals that the edges of the particles are getting more indistinct, and the cubes tend to transform into spheres with the addition steps (divided shares) increasing. The more the stages divided, the closer the concentration of $Ca^{2+}$ and $CO_3^{2-}$ is to the equilibrated concentration and the more beneficial is to the formation of metastable spherical $CaCO_3$ crystals. It can be speculated that, to obtain spherical $CaCO_3$ crystals, more addition steps (divided shares) of $Na_2CO_3$ powders or using $Na_2CO_3$ solution are necessary.

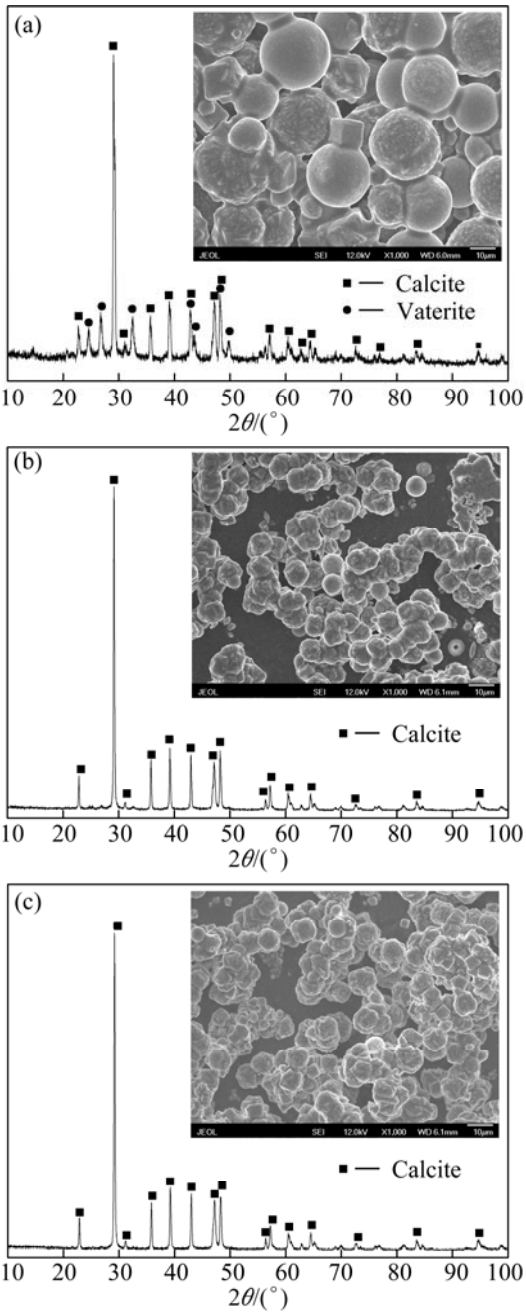


**Fig. 8** SEM images and XRD patterns of calcium carbonate at different equilibrium time: (a) 0 h; (b) 4 h; (c) 10 h (Concentration 0.6 mol/L; Flow rate 1 mL/min; Reaction temperature: 20 °C; Stirring speed: 200 r/min)

**3.5 Technology improvement**

The above physical and chemical analyses show that the soluble salts dissolved into the leaching solution during the leaching process mainly exist in the form of potassium chloride, sodium chloride, calcium sulfate and potassium sulfate, while ferric oxide is the main component of the residue. The recovery experiment indicates that the recovery process is feasible and there is almost no secondary pollution produced in the whole recovery process. Recovering potassium from ESP dust is a potential and unusual method, due to large output, low cost, simple operation and easy industrialization. The process in patent [3] was redesigned for KCl production with joint production of spherical calcium carbonate (see Fig. 10). Mixing the sintering dust with water in the pre-leaching tank and transiting the mixture solution into the leaching tank for the further leaching; then filtering the leaching solution after some time; thirdly, adding the sodium carbonate solution into the filtrate solution; then filtering the solution and the spherical calcium carbonate product can be obtained; finally, evaporating the purified filtrate step by step to obtain the high purity KCl and $K_2SO_4$ products.

## 4 Conclusions

1) ICP-AES, XRD and SEM−EDS results show that K in the ESP dust mostly exists in the form of KCl, which can be separated easily from the dust by water leaching.

2) A lower liquid−solid ratio should be chosen in the leaching process to inhibit the dissolution of calcium sulfate dehydrate. The low liquid−solid ratio in actual production not only reduces the dissolution of calcium ions from the sintering dust, but also decreases the precipitant consumption in the precipitation process and saves energy in the evaporation crystallization process.

3) Almost 100% of $Ca^{2+}$ can be removed using sodium carbonate as the precipitating agent. Spherical calcium carbonate with mean particle size of 10 μm can be obtained at the following conditions: less than 1.3 mol/L sodium carbonate solution is pumped with the flow of 1 mL/min into the leaching solution, and

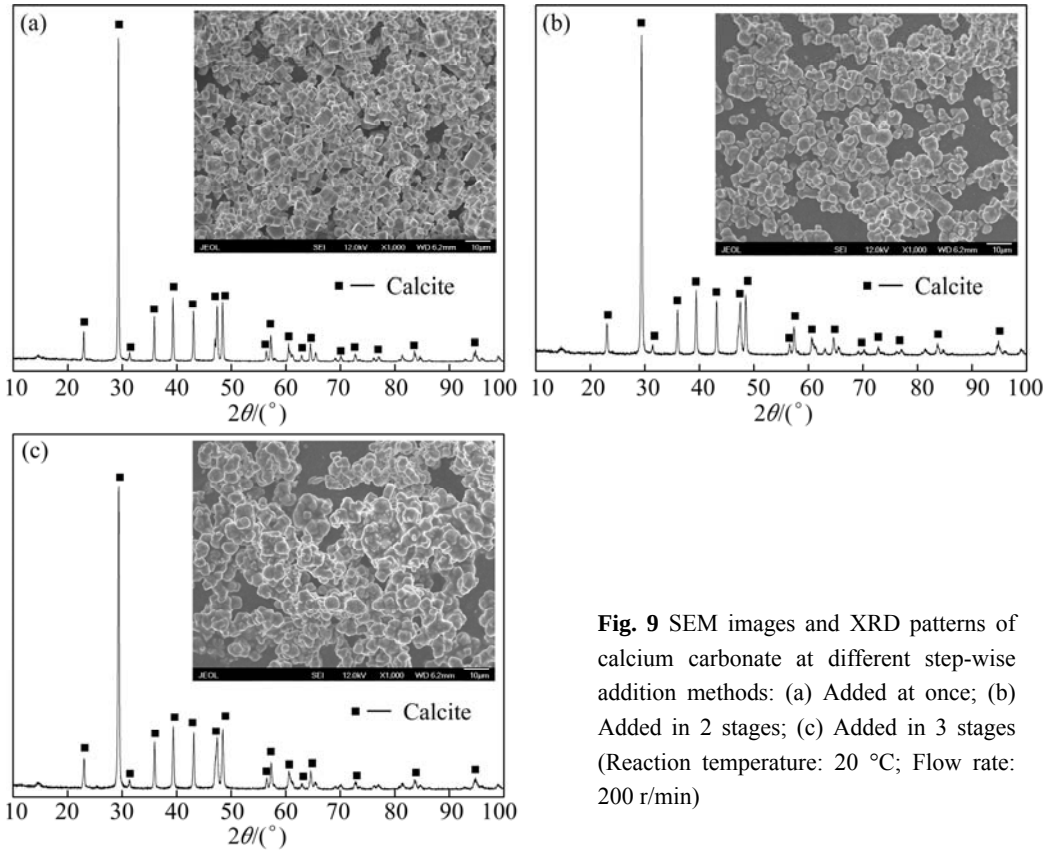


**Fig. 9** SEM images and XRD patterns of calcium carbonate at different step-wise addition methods: (a) Added at once; (b) Added in 2 stages; (c) Added in 3 stages (Reaction temperature: 20 °C; Flow rate: 200 r/min)

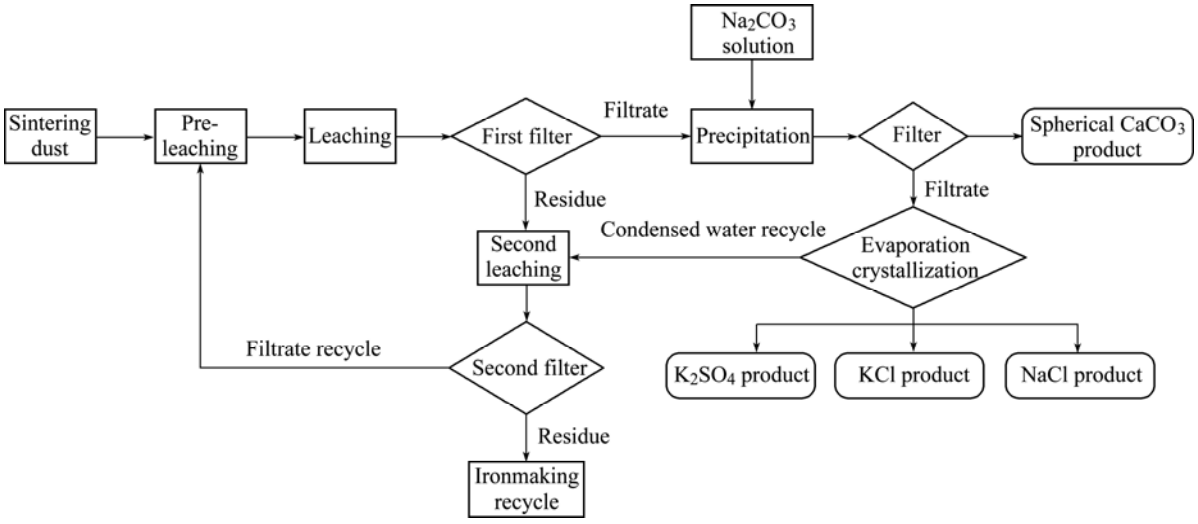


**Fig. 10** Process flow of KCl production with joint production of spherical calcium carbonate

reaction temperature and stirring speed are 20 °C and 200 r/min.

4) The potassium recovery process with joint production of spherical calcium carbonate was designed as follows: leaching the sintering dust with water at a certain temperature for some time, then filtering the leaching solution, producing the spherical calcium carbonate from the filtrate by adding sodium carbonate solution, finally, evaporating the purified filtrate step by step to obtain the high purity products of KCl and $K_2SO_4$.

## References


[1] BAO Rong-hua. China should adopt various countermeasures with the intensification of the monopoly on world-wide potash industries [J]. Land and Resources Information, 2012(7): 26−28. (in Chinese)

[2] WANG Jie. The lowest price in the world: China won the import contract for potash [N]. 21st Century Business Herald, 2012−03−22(17). (in Chinese)

[3] GUO Zhan-cheng, PENG Cui, ZHANG Fu-li, PAN Zhao-bin. Utilization of sintering dust of iron and steel enterprise for producing potassium chloride: China, 200810101269 [P]. 2008−03−03. (in Chinese)

[4] ZHAN Guang, GUO Zhan-cheng. Basic properties of sintering dust from iron and steel plant and potassium recovery [J]. Journal of Environmental Sciences, 2013, 25(6): 1226−1234.

[5] ZHAN Guang, GUO Zhan-cheng. Water leaching kinetics and recovery of potassium salt from sintering dust [J]. Transactions of Nonferrous Metals Society of China, 2013, 23(12): 3770−3779.

[6] WANG Hong-qing, BAO Zong-hong, DUAN Dong-ping, LI Zhi-bao, KE Jia-jun, DEMOPOULOS G P. Inhibition of calcium sulfate scale formation in pipes of brine [J]. The Chinese Journal of Nonferrous Metals, 2008, 18(S1): 92−95.(in Chinese)

[7] ELKANZI E M, CHALABI M F. Kinetics of the conversion of calcium sulfate to ammonium sulfate using ammonium carbonate aqueous solution [J]. Industrial & Engineering Chemistry Research, 1991, 30(6): 1289−1293.

[8] WANG Xian-hua. Research on brine purification and utilization of purified calcium and magnesium [J]. China Well and Rock Salt, 2011, 42(5): 5−7. (in Chinese)

[9] CHEN Xian-yong, TANG Qin, HU Wei-bing, DAN You-meng, ZHOU Gui-yun. Preparation and characterization of twin spherical calcium carbonate by the direct mixing precipitation method [J]. Chemical Journal of Chinese Universities, 2010, 31(10): 1940−1944. (in Chinese)

[10] DING Tao, LU Shou-ci, DU Gao-xiang. Mechano-activated surface modification of calcium carbonate in wet stirred mill and its properties [J]. Transactions of Nonferrous Metals Society of China, 2007, 17(5): 1100−1104.

[11] WALSH D, LEBEAU B, MANN S. Morphosynthesis of calcium carbonate (vaterite) microsponges [J]. Advanced Materials, 1999, 11(4): 324−328.

[12] AJIKUMAR K P, LAKSHMINARAYANAN R, VALIYAVEETTIL S. Controlled deposition of thin films of calcium carbonate on natural and synthetic templates [J]. Crystal Growth & Design, 2004, 4(2): 331−335.

[13] JORG K, SESHADRI R, KNOLL W, TREMELL W. Templated growth of calcite, vaterite and aragonite crystals onself-assembled monolayers of substituted alkylthiols on gold [J]. Journal of Materials Chemistry, 1998(8): 641−650.

[14] LOSTE E, MARTI D E, ZARBAKHSH A, MELDRUM C F. Study of calcium carbonate precipitation under a series of fatty acid Langmuir monolayers using Brewster angle microscopy [J]. Langmuir, 2003, 19(7): 2830−2837.

[15] QI Li-min, LI Jie, MA Ji-ming. Biomimetic morphogenesis of carbonate in mixed solutions of surfactants and double-hydrophilic block copolymers [J]. Advanced Materials, 2002, 14(4): 300−303.

[16] ZHANG Qun, FANG Liang, CHEN Chuan-bao. Design and synthesis of calcium carbonate microsphere by the synergistic effect of poly (sodium 4-styene-sulfonate) and L-glutamic acid [J]. Chinese Journal of Inorganic Chemistry, 2008, 24(4): 553−559. (in Chinese)

[17] LIU Qing-fang, CHEN Shou-tian, LIU Qian. Effect of experiment parameters on the crystalline habit of calcium carbonare whisker [J]. Journal of Inorganic Materials, 2002, 17(1): 163−166. (in Chinese)

[18] Inorganic Chemistry Department of Dalian University of Technology. Inorganic chemistry [M]. Beijing: Higher Education Press, 2001. (in Chinese)

[19] WU Xiao-qin, HE Wei, GUAN Bao-hong, WU Zhong-biao. Solubility of calcium sulfate dihydrate in Ca−Mg−K chloride salt solution in the rang of (348.15 to 371.15) K [J]. Journal of Chemistry & Engineering Data, 2010, 55(6): 2100−2107.

[20] HE Wei, WU Xiao-qin, LIU Fang. Calcium sulfate solubilities in the Ca−Mg−K−Cl−$H_2O$ system of transformation process [J]. Environmental Sciences & Technology, 2010, 33(5): 35−38. (in Chinese)

[21] LIANG Ying-jiao. Data handbook of the thermodynamic properties for the inorganic substances [M]. Shenyang: Northeastern University Press, 1993. (in Chinese)

[22] PENG Cui, ZHANG Fu-li, GUO Zhan-cheng. Gypsum crystallization and potassium chloride regeneration by reaction of calcium chloride solution with potassium sulfate solution or solid [J]. Transactions of Nonferrous Metals Society of China, 2010, 20(4): 712−720.

[23] YANG Shan-rang, CAO Sheng-xian, CHEN Li-jun, YU Ming-le, SUN Wei-hua, XU Zhi-ming. A study on the conductimetric titration of the calcium carbonate fouline induction period [J]. Journal of Engineering Thermophysics, 2008, 29(9): 1577−1580. (in Chinese)

[24] ZOU Kong-biao, WANG Wei, LU Wen-qing, NIE Su-yun. Synthesis of spherical $CaCO_3$ by polyvinyl alcohol as additive [J]. Journal of Nanjing Normal University: Engineering and Technology Edition, 2008, 8(1): 64−68. (in Chinese)

[25] XIE Yuan-yan, YANG Hai-lin, RUAN Jian-ming, ZHOU Zhong-cheng. Preparation of calcium carbonate whiskers by sol-gel method [J]. Materials Science and Engineering of Powder Metallurgy, 2009, 14(3): 164−168. (in Chinese)

# 烧结电除尘灰浸出液中回收钾盐及联产球形碳酸钙

詹 光，郭占成

北京科技大学 钢铁冶金新技术国家重点实验室，北京 100083

**摘 要**：采用一些物理化学表征手段对包钢烧结电除尘灰的基础性质进行研究。结果表明，该烧结电除尘灰的主要成分为 KCl、NaCl、$Fe_2O_3$ 和 $Fe_3O_4$。烧结电除尘灰的水浸实验表明，烧结电除尘灰中的氯化钾可以通过水浸蒸发的方式回收。浸出液分析结果表明，浸出液中含有大量可溶性硫酸钙。为了获得纯净的氯化钾产品，这些可溶性硫酸钙需要事先进行去除。为了提供抑制硫酸钙从烧结电除尘灰中浸出溶解的理论数据指导，开展了烧结电除尘灰的浸出实验和硫酸钙在 KCl、NaCl、$K_2SO_4$ 及其混合盐中的溶解性能实验。结果表明，在浸出过程中，采用小的液固比能很好地抑制烧结电除尘灰中硫酸钙的溶解。研究碳酸钠沉淀剂的浓度、反应温度、搅拌强度和平衡时间对制备球形碳酸钙的影响。获得了分散良好，粒径尺寸小于 10 μm 的球形碳酸钙。同时，设计了一个从烧结电除尘灰提取氯化钾并联产球形碳酸钙副产品的工艺路线。该工艺技术可行，经济效益较好。

**关键词**：烧结电除尘灰；钾盐；回收实验；球形碳酸钙

**(Edited by Xiang-qun LI)**